Volume 10 | Issue 4 Article 7

Bacterial Cellulose Production from Fermented Fruits and Vegetables Byproducts: A Comprehensive Study on Chemical and Morphological Properties

Yati Maryati
Research Center for Chemistry-National Research and Innovation Agency (BRIN), Serpong, Tangerang Selatan, Banten, Indonesia

Hakiki Melanie
Research Center for Chemistry-National Research and Innovation Agency (BRIN), Serpong, Tangerang Selatan, Banten, Indonesia

Windri Handayani
Department of Biology, Faculty of Mathematics and Natural Sciences, Universitas Indonesia, Depok, Jawa Barat, Indonesia

Yasman Yasman
Department of Biology, Faculty of Mathematics and Natural Sciences, Universitas Indonesia, Depok, Jawa Barat, Indonesia, yasman.si@sci.ui.ac.id

Recommended Citation

Maryati, Yati; Melanie, Hakiki; Handayani, Windri; and Yasman, Yasman (2024) "Bacterial Cellulose Production from Fermented Fruits and Vegetables Byproducts: A Comprehensive Study on Chemical and Morphological Properties," *Karbala International Journal of Modern Science*: Vol. 10 : Iss. 4 , Article 7.
Available at: https://doi.org/10.33640/2405-609X.3376

Bacterial Cellulose Production from Fermented Fruits and Vegetables Byproducts: A Comprehensive Study on Chemical and Morphological Properties

Abstract

This study aimed to produce α-cellulose from Bacterial Cellulose SCOBY (BCS) using alternative substrates from fermented fruit and vegetable byproducts: *katuk* leaves (KT), *kale* leaves (KL), guava (JB), dragon fruit (NG), and banana (PS). BCS production involved juice extraction, SCOBY inoculation, and sucrose addition, followed by 21 days of fermentation. Initially, the NG medium had the highest concentration of Total Reducing Sugars (TRS), but all media showed a decline as sugars were consumed. Fermentation reduced pH and increased total polyphenols, with KL and JB showing the highest rise (0.13-0.15 mg GAE/mL). Flavonoid levels varied, decreasing in KL and PS but increasing in KL, JB, and NG. Antioxidant activity decreased in NG (13.21%), while KL increased by 43.49%. BCS characteristics varied, with KL producing the thickest BCS (3.41±0.40 mm wet, 0.73±0.06 mm dry). The JB medium yielded the highest dry BCS (17.20±1.86%), with lower water content (81.13±1.71%). XRD analysis after alkali treatment revealed increased crystallinity in α-BCS, with crystallite sizes of 4.78 to 8.40 nm, larger than standard α-cellulose. α-BCS from kale showed higher DMSO compatibility than water. These results demonstrate the diverse properties of BCS from alternative substrates, highlighting potential industrial and biomedical applications.

Keywords

-cellulose, Bacterial Cellulose SCOBY, alternative substrates, fermented beverages, physicochemical and morpho-logical properties.

RESEARCH PAPER

Bacterial Cellulose Production From Fermented Fruits and Vegetables Byproducts: A Comprehensive Study on Chemical and Morphological Properties

Yati Maryati [a,b], Hakiki Melanie [a], Windri Handayani [b,c], Yasman Yasman [b,c,*]

[a] Research Center for Chemistry-National Research and Innovation Agency (BRIN), Serpong, Tangerang Selatan, Banten, Indonesia
[b] Department of Biology, Faculty of Mathematics and Natural Sciences, Universitas Indonesia, Depok, Jawa Barat, Indonesia
[c] Research Group of Metabolomics and Chemical Ecology, Department of Biology, Faculty of Mathematics and Natural Sciences, Universitas Indonesia, Depok, Jawa Barat, Indonesia

Abstract

This study aimed to produce α-cellulose from Bacterial Cellulose SCOBY (BCS) using alternative substrates from fermented fruit and vegetable byproducts: *katuk* leaves (KT), *kale* leaves (KL), guava (JB), dragon fruit (NG), and banana (PS). BCS production involved juice extraction, SCOBY inoculation, and sucrose addition, followed by 21 days of fermentation. Initially, the NG medium had the highest concentration of Total Reducing Sugars (TRS), but all media showed a decline as sugars were consumed. Fermentation reduced pH and increased total polyphenols, with KL and JB showing the highest rise (0.13−0.15 mg GAE/mL). Flavonoid levels varied, decreasing in KL and PS but increasing in KL, JB, and NG. Antioxidant activity decreased in NG (13.21%), while KL increased by 43.49%. BCS characteristics varied, with KL producing the thickest BCS (3.41 ± 0.40 mm wet, 0.73 ± 0.06 mm dry). The JB medium yielded the highest dry BCS (17.20 ± 1.86%), with lower water content (81.13 ± 1.71%). XRD analysis after alkali treatment revealed increased crystallinity in α-BCS, with crystallite sizes of 4.78−8.40 nm, larger than standard α-cellulose. α-BCS from kale showed higher DMSO compatibility than water. These results demonstrate the diverse properties of BCS from alternative substrates, highlighting potential industrial and biomedical applications.

Keywords: α-cellulose, Bacterial cellulose SCOBY, Alternative substrates, Fermented beverages, Physicochemical and morphological properties

1. Introduction

The escalating demand for plant cellulose derivatives has increased the reliance on wood as a primary raw material, with substances like carboxymethyl cellulose (CMC), hydroxyethyl cellulose (HEC), cellulose acetate, and methyl cellulose used across industries such as food, pharmaceuticals, biomedicine, chemistry, and textiles. This reliance poses environmental risks like deforestation [1]. To address these concerns, biodegradable materials promoted through green chemistry aim to reduce dependence on fossil fuels [2].

While plants are the main cellulose source, certain bacteria produce bacterial cellulose (BC), which is purer than plant-derived cellulose. BC is synthesized by bacterial strains such as *Acetobacter*, *Komagataeibacter*, and *Lactobacillus* [3]. BC has a fibrillar and semi-crystalline structure due to its molecular bonding [4], and sustainable production can be achieved using agricultural waste [5,6].

BC can also be produced as a byproduct of kombucha fermentation using symbiotic cultures of bacteria and yeast (SCOBY), displaying mechanical and physicochemical properties suitable for industries like food and textiles [7,8]. The production

Received 7 August 2024; revised 28 September 2024; accepted 1 October 2024.
Available online 5 November 2024

* Corresponding author at: Department of Biology, Faculty of Mathematics and Natural Sciences, Universitas Indonesia, Depok, Jawa Barat, Indonesia.
E-mail address: yasman.si@sci.ui.ac.id (Y. Yasman).
Peer review under responsibility of University of Kerbala.

https://doi.org/10.33640/2405-609X.3376

of 79.2 tons of BC in 22 days from a 500,000 L setup demonstrates its efficiency, compared to plant cellulose yields [9].

BC synthesis from SCOBY involves acetic acid bacteria and yeast, with population variations influenced by geographical and environmental factors [10–13]. The bacteria polymerize sugars into cellulose, while lactic acid bacteria maintain microbiological conditions [12,14–18]. Pure cultures struggle to achieve this balance because bacteria and yeast cannot function optimally in isolation [19]. SCOBY offers a more practical solution for large-scale production, eliminating the need to maintain separate bacterial and yeast strains for ideal fermentation conditions. Furthermore, SCOBY maintenance is more cost-effective and a by-product of kombucha production, potentially reducing expenses compared to methods using specialized cellulose culture media [20]. To maintain consistent quality in SCOBY bacterial cellulose production, fermentation optimization techniques are employed by adjusting the temperature, pH, and nutrients. The use of automatic controls in bioreactors also enhances the consistency of cellulose production [21,22].

The structural development of SCOBY-derived cellulose is impacted by polyphenols in tea, as well as fruits and vegetables, which enhance antioxidant properties [23–25]. SCOBY-based BC (BCS) offers health benefits such as water retention, low-calorie fiber content, and safety approval by the FDA [15,26–29].

Developing cost-effective BC production methods using agricultural byproducts is crucial for industrial applications [9,28–31]. Various agricultural sources, including wheat bran, grape extract, coffee cherry husks, and fruits like pineapple and watermelon, have been found effective for BC synthesis [32–34]. This approach aligns with sustainability goals and promotes large-scale BC production.

Building on research showing kombucha can enhance phenolic content and antioxidant capacity in fermented substrates [35–37], this study explores the use of SCOBY biomass for BC production using substrates from fermented vegetables and fruits like *katuk* leaves, *kale* leaves, guava, banana and dragon fruit.

2. Materials and methods

2.1. Preparing the starter culture for kombucha SCOBY

The initial step involved creating a nutrient-rich foundation for fermentation by preparing sweet tea solution. This was achieved by dissolving 10% w/v sugar in hot water followed by steeping 3% w/v green tea. Subsequently, commercial SCOBY (10% v/v liquid portion and 5% commercial SCOBY pellicle) was added to the sweetened tea, which was crucial for introducing the necessary microbial diversity [38]. The mixture was then placed in a container, covered, and left to ferment at room temperature (27–30 °C) for 21 d. During this period, SCOBY grows, rises to the surface, and forms a thin layer.

2.2. Medium and growth bacterial cellulose SCOBY production

Juices were extracted from guava, banana, and dragon fruit harvested at 75% ripeness. For banana and dragon fruit, the skins were removed, and the pulp was mixed with sterile water in a 1:6 ratio before blending. For green leafy vegetables like *katuk* and *kale*, the stems were removed during cleaning, and the leaves were blended with sterile water at a 1:10 ratio. Each sample was then filtered to produce fruit or vegetable juice, followed by an additional filtration through a 60-mesh sieve to obtain the final filtrates. Subsequently, the obtained filtrates underwent pasteurization at 90–100 °C for 5–10 min. Following pasteurization, which had an initial pH of approximately 5–6, was inoculated with a SCOBY starter culture (Kombuchaforever) consisting of 10% v/v acid liquid and 5% SCOBY pellicle and supplemented with 10% w/v sucrose and enriched with 10% w/v of sucrose. Fermentation was conducted at room temperature (27–30 °C) for 21 days. Post-fermentation, the separated filtrates underwent a comprehensive analysis of their chemical properties. This included the determination of protein content using the Lowry method [39], analysis of total reducing sugars (TRS) via the dinitrosalicylic acid (DNS) method [40], as well as assessment of phenolic content [41], flavonoid content [42], DPPH antioxidant activity [43], and pH value [44]. The byproduct of this fermentation process, recognized as Bacterial Cellulose from SCOBY (BCS), was collected and subsequently subjected to analysis. The obtained BCS underwent a thorough examination, including measurements of thickness. The thickness of each BCS membrane was measured at various positions using a thickness gauge (Mitutoyo micrometer), and the resulting values were averaged, assessment of moisture content, determination of yield [45], and calculation of average production [46]. For morphological characterization, Field-Emission Scanning Electron Microscope (FE-SEM) was employed, and cellulose fiber diameters were quantitatively measured using *ImageJ* software. This detailed process aimed to

provide a comprehensive understanding of the properties and characteristics of Bacterial Cellulose from SCOBY derived from diverse fruit and vegetable substrates, calculated using Equations (1–3).

$$\text{BCS productivity } \left(g.L^{-1}.d\right) = M_1/(V.\,t) \quad (1)$$

$$\text{Wet BCS Yield } \left(g.L^{-1}\right) = M_0/V \quad (2)$$

$$\text{Dry BCS Yield } \left(g.L^{-1}\right) = M_1/V \quad (3)$$

where (M_0) is the amount of the produced wet BCS (g), (M_1) is the amount of the produced dry BCS (g), (V) is the production volume (L), and (t) is the fermentation time (days).

2.3. Isolation of α-bacterial cellulose from SCOBY (α-BCS)

The process commenced by isolating BCS from each fermented vegetable and fruit substrate, followed by a thorough washing with running water. Afterward, the BCS underwent a drying phase at 50 °C for 48 h. The resulting dried BCS mass underwent further refinement through blending to reduce particle size. Subsequently, the BCS powder underwent boiling in hot water, filtration, and subsequent separation into soluble and insoluble components.

Advancing in the process, purification took center stage, focusing on the elimination of any residual cellular residues. This purification step involved treating the residue with 2% NaOH for 15 min at 100 °C, followed by meticulous washing with deionized water until achieving a neutral pH range of 6–7. The residue then underwent soaking in 17.5% NaOH for 10–15 min, followed by separation through filtration. Additional washing with deionized water was conducted until reaching a pH of 6–7. The resultant residue, referred to as α-BCS, was subsequently dried in an oven at 50 °C.

2.4. Characterization α-BCS

The meticulous sequence of steps ensured a comprehensive characterization of α-BCS, emphasizing its purity and structural properties. Functional groups of α-BCS were identified through Fourier-transform infrared spectroscopy (FTIR) using a Bruker Tensor II instrument with an ATR accessory, covering the frequency range of 4000–500 cm^{-1}. ATR-FTIR spectroscopy employs an ATR crystal to direct infrared light at a specific angle, causing internal reflection and generating an evanescent wave that briefly penetrates the sample in contact with the surface of the crystal [47]. This interaction produces a spectrum revealing molecular vibrations, thereby identifying the chemical bonds and functional groups in the material [48].

The degree of α-BCS crystallinity was determined using X-ray diffraction (XRD) with a RIGAKU SMARTLAB Instrument, employing monochromatic Cu Kα radiation (λ = 1.54059 Å) at 40 kV and 30 mA, with a scanning speed of 10°/min. The XRD pattern was scanned from 10 to 50° (2θ) with a step interval of 0.02°. When X-rays interact with a sample, a portion of the rays undergo diffraction by atoms within the crystal structure, resulting in a distinctive diffraction pattern [49]. The angle of diffraction is measured to determine the spacing between atomic layers in the crystal, which can be utilized to calculate the crystal grain size using the Scherrer equation [50]. The determination of the cellulose crystallinity index from the XRD spectrum was calculated using the peak height method, according to the Segal Equation (4) [51–53]. In this method, the Crystallinity Index (CI) is calculated as the ratio of the peak intensity of the crystalline region (I_{002} - I_{AM}) to the total intensity (I_{002}) after subtracting the background signal measured without cellulose [54].

$$CI\,(\%) = (I_{002} - I_{AM})\,/\,I_{002}\,x\,100\% \quad (4)$$

Where: CI = Crystallinity Index; I_{002} = Intensity of the crystalline region at 2θ (≈22.5); I_{AM} = Intensity of the amorphous region at 2θ (≈18.3).

The crystallite size (CrS) is calculated using the Debye Scherrer's Equation (5):

$$CrS = k.\lambda/(FWHM\cos\Theta) \quad (5)$$

Where (k) is the dimensionless Scherrer constant, which equals 0.9, (λ) is the wavelength of X-ray diffraction, (FWHM) is the full width at half maximum in radians, and (Θ) is the diffraction angle in radians.

2.5. Liquid holding capacity (LHC)

The dry α-BCS powder (0.150 g) was immersed in a solvent consisting of 6 g of distilled water (H_2O) and dimethyl sulfoxide (DMSO). The suspension was allowed to stand for 24 h. Following this period, the sample was centrifuged at 5000 rpm for 10 min, and any excess water was carefully discarded. The sample was then re-weighed, and its mass (W_1) was duly recorded. Subsequently, the sample underwent drying in an oven at 60 °C until a consistent weight (W_0) was attained, following the methodology outlined in 2019 by Ref. [55]. The entire

experiment was conducted in triplicate to ensure robust and reliable results. The water absorption (%) was calculated based on Equation (6):

$$\text{LHC}\ (\%) = [(W_1 - W_0) / W_0] \text{x}\ 100\% \quad (6)$$

Where W_1 is the dry weight of α-BCS (g), W_0 is the wet weight of α-BCS (g).

2.6. Statistical analysis

Statistical analysis of the data was conducted using Minitab Statistical Software, Release 16 for Windows. The methods employed were One-way analysis of variance (ANOVA) and Tukey's HSD (Honestly Significant Difference) test, with statistical significance set at $p < 0.05$.

3. Result and discussions

The chemical composition of fruit and vegetable extracts in kombucha fermentation varied depending on the specific fruit and vegetable used. Both fruits and vegetables provided sugars as energy sources for microorganisms, including yeast and acetic acid bacteria, and contribute to the distinct aroma and flavor profiles of kombucha. Additionally, fruits and vegetables contained bioactive compounds such as flavonoids, polyphenols, and other phytochemicals, which enhanced flavor and may offer health benefits. Elfirta et al. (2024) reported that the type of substrate contributed to the production of phenolic and flavonoid compounds during fermentation, enhancing antioxidant activity [56]. These chemical intricacies are outlined in Table 1, which provides a comprehensive overview of the fermentation process.

The evaluation results showed significant composition differences among the five fermentation media ($p < 0.05$). Dragon fruit (NG) had the highest TRS content at 16.98 mg/mL, followed by guava (JB) and banana (PS), while *katuk* (KT) had the lowest TRS content at 1.87 mg/mL. All media experienced a decline in TRS content during the 21-day fermentation, with guava (JB) exhibiting the most significant reduction (ΔTRS) at 8.42 mg/mL, followed by banana (PS) and dragon fruit (NG), while *kale* (KL) had the lowest ΔTRS at 1.86 mg/mL. This reduction was due to simple sugars, primarily sucrose, serving as a carbon source for microorganisms. As fermentation progressed, sugars transformed into organic acids [11], correlating with pH reduction. The initial pH of kombucha ranged from 2.92 to 3.40, showing further reduction during fermentation. Excessive pH decrease disrupted microbial growth, emphasizing pH control's importance [57,58]. Significant differences in soluble protein content were observed ($p < 0.05$), influenced by raw material composition. Protein content remained relatively stable during fermentation. Shifts were noted in *kale* (KL) and dragon fruit (NG) media, with minor variations attributed to microbial activities [59,60]. Fruit and vegetable kombucha fermentation significantly influenced polyphenolic compounds and flavonoids ($p < 0.05$). While total polyphenols increased, specific flavonoid levels varied due to fermentation intricacies and microbial activity [61]. Antioxidant activity consistently demonstrated significant impact ($p < 0.05$) during fermentation, with prolonged fermentation decreasing activity due to compound degradation [62,63]. Additionally, microbial activity within kombucha broke down antioxidant compounds into less active forms, thereby diminishing the overall effectiveness of the antioxidants in combating oxidation, as elucidated by Ref. [64].

The fermentation process of kombucha significantly influences the content of sugar, pH, protein,

Table 1. Transformation of chemical properties in fruit and vegetable medium before and after fermentation.

	Time of fermentation (days)	Medium				
		KT	KL	JB	NG	PS
Total reducing sugar (TRS) (mg/mL)	0	4.44 ± 0.25^{d}	3.12 ± 0.14^{d}	11.67 ± 0.25^{b}	16.98 ± 1.03^{a}	8.46 ± 0.26^{c}
	21	1.87 ± 0.13^{bc}	1.26 ± 0.06^{c}	3.25 ± 0.11^{b}	11.33 ± 5.37^{a}	2.72 ± 0.04^{b}
Protein (mg/mL)	0	4.59 ± 0.20^{a}	1.51 ± 0.20^{d}	2.69 ± 0.25^{b}	2.15 ± 0.11^{bc}	1.96 ± 0.07^{cd}
	21	4.22 ± 0.03^{a}	3.15 ± 0.02^{ab}	3.34 ± 0.16^{ab}	3.82 ± 1.06^{a}	1.50 ± 0.03^{b}
pH	0	3.40 ± 0.09^{a}	3.26 ± 0.01^{a}	2.92 ± 0.02^{b}	3.30 ± 0.03^{a}	3.22 ± 0.03^{a}
	21	3.28 ± 0.02^{a}	3.11 ± 0.09^{a}	1.99 ± 0.01^{c}	1.85 ± 0.01^{c}	2.65 ± 0.05^{b}
Total polyphenol (mg GAE/mL)	0	0.35 ± 0.10^{a}	0.16 ± 0.00^{b}	0.28 ± 0.01^{a}	0.17 ± 0.03^{b}	0.24 ± 0.04^{ab}
	21	0.42 ± 0.03^{ab}	0.29 ± 0.00^{bc}	0.44 ± 0.13^{a}	0.22 ± 0.04^{c}	0.29 ± 0.02^{bc}
Flavonoid (μg/mL)	0	1118.20 ± 40.01^{d}	102.50 ± 1.13^{b}	225.20 ± 1.84^{c}	13.90 ± 1.70^{a}	333.00 ± 11.17^{cd}
	21	965.70 ± 10.18^{d}	183.20 ± 3.54^{b}	367.00 ± 1.27^{c}	54.30 ± 1.41^{a}	136.00 ± 14.00^{b}
Antioxidant DPPH (%inhibition)	0	88.23 ± 1.25^{a}	38.64 ± 1.98^{c}	85.86 ± 3.54^{a}	57.57 ± 2.83^{b}	85.39 ± 1.94^{a}
	21	79.05 ± 3.63^{a}	55.44 ± 1.82^{b}	81.56 ± 4.68^{a}	49.96 ± 1.56^{b}	84.04 ± 0.09^{a}

[a,b,c,d] The mean values followed by different letters in the same row indicate significant differences ($p < 0.05$).

polyphenol compounds, flavonoids, and antioxidant activity, with these alterations closely associated with the activity of microorganisms during fermentation. The influence of phenolic compounds and flavonoids on bacterial cellulose production is complex and varies based on factors such as the type and quantity of compounds, bacterial strains, and environmental conditions. Generally, low concentrations of these substances are advantageous, whereas high concentrations may suppress their production. Studies have demonstrated that increasing the bioactive components in growth media can enhance bacterial cellulose synthesis. Lima et al. (2023) discovered that higher levels of sucrose and kombucha in culture media led to increased total phenolic compounds and flavonoids, thereby enhancing bacterial cellulose production [65]. Kim et al. (2023) observed that fermenting specific combinations of acetic acid bacteria and yeast increased total phenolic and flavonoid content, improving the antioxidant properties of kombucha [66]. Certain phenolic compounds, such as catechins and gallic acid, are associated with increased cellulose production owing to their involvement in metabolic pathways that support bacterial growth and cellulose synthesis. Furthermore, Tapias et al. (2022) reported that polyphenol-rich herbal infusions enhance the antioxidant activity of bacterial cellulose films, suggesting a synergistic effect on cellulose production [6]. However, some phenolic compounds can inhibit bacterial growth. Zhang et al. (2014) discovered that coniferyl aldehyde and vanillin significantly impede the growth of *Gluconacetobacter xylinus*, which is the primary bacterium responsible for BC production [67]. Coniferyl aldehyde completely inhibited BC production at low concentrations, while vanillin reduced BC yield by approximately 60% at higher concentrations.

All five types of kombucha media (comprising fruits and vegetables) that underwent a 21-day fermentation period demonstrated the capacity to generate BCS pellicles on the liquid surface. The overall morphology of both wet and dry BCS products is visually depicted in Fig. 1.

The thickness of each BCS membrane was measured at various positions using a thickness gauge, and the resulting values were averaged. Comparative analysis of the wet and dry thickness values revealed significant differences in the growth capability of BCS across the five media ($p < 0.05$) (Table 2). The banana (PS) and *kale* (KL) media exhibited the highest wet and dry thickness values, along with the highest average productivity of BCS, signifying superior growth capability. Following closely were the guava (JB) and *katuk* (KT) media, while the dragon fruit (NG) medium displayed the lowest thickness values. Moisture content exhibited significant variations across all five media ($p < 0.05$),

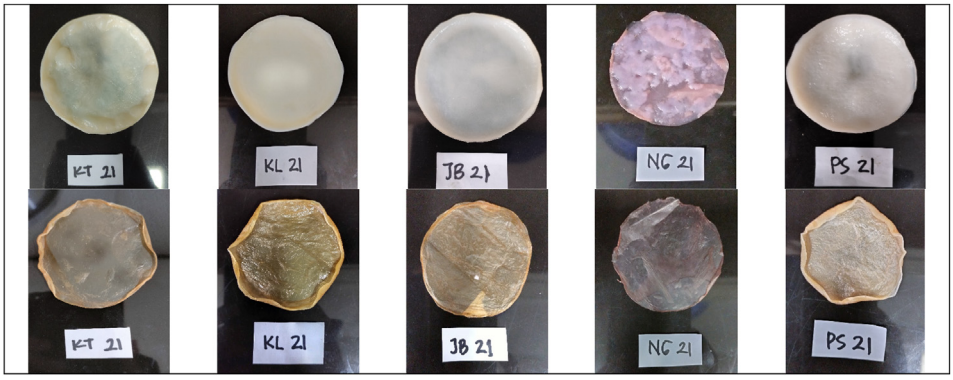

Fig. 1. Morphological characteristics of produced films: Wet BCS (upper row) and dry BCS (lower row), derived from fruit and vegetable fermentation byproducts.

Table 2. Physical properties of BCS kombucha byproducts derived from fruits and vegetables following a 21-day fermentation period.

Medium	Wet Thickness (mm)	Dry Thickness (mm)	Moisture%	Wet BCS Yield ($g.L^{-1}$)	Dry BCS Yield ($g.L^{-1}$)	Productivity ($g.L^{-1}.d$)
KT	1.61 ± 0.30^{c}	0.46 ± 0.20^{b}	89.61 ± 0.83^{ab}	87.00 ± 8.58^{b}	9.04 ± 1.20^{c}	0.43 ± 0.02^{c}
KL	3.41 ± 0.40^{b}	0.73 ± 0.06^{a}	87.11 ± 0.63^{b}	117.39 ± 17.93^{a}	15.10 ± 2.58^{ab}	0.72 ± 0.04^{ab}
JB	1.52 ± 0.06^{cd}	0.41 ± 0.09^{b}	81.13 ± 1.71^{c}	90.36 ± 3.31^{b}	17.20 ± 1.86^{a}	0.82 ± 0.01^{a}
NG	0.85 ± 0.11^{d}	0.15 ± 0.02^{c}	90.13 ± 1.37^{a}	48.31 ± 6.70^{c}	5.04 ± 0.18^{d}	0.24 ± 0.15^{d}
PS	4.31 ± 0.37^{a}	0.72 ± 0.07^{a}	87.08 ± 2.02^{b}	95.58 ± 12.40^{b}	12.35 ± 2.66^{b}	0.22 ± 0.03^{b}

[a,b,c,d] The average values followed by different letters in the same column indicate a significant difference ($p < 0.05$).

impacting the resulting yield. The dragon fruit (NG) medium yielded the highest moisture content in the BCS pellicle, registering at 90.13 ± 1.37%, while the guava (JB) medium recorded the lowest at 81.13 ± 1.71%. The *kale* (KL) medium demonstrated the highest wet BCS yield, directly correlating with the wet BCS thickness, with a value of 117.39 ± 17.93 g/L, while the dragon fruit (NG) medium displayed the lowest wet BCS yield at 48.31 ± 6.70 g/L (Table 2). Conversely, the dry BCS yield exhibited an inverse relationship with moisture content. Higher moisture content resulted in lower dry BCS yield and vice versa. The guava (JB) medium yielded the highest dry BCS yield at 17.20 ± 1.86 g/L, whereas the dragon fruit (NG) medium recorded the lowest at 5.04 ± 0.18 g/L.

According to Ref. [68], the biomass yield is influenced by the characteristics of the substrate, which was also demonstrated in this study. Wet and dry bacterial cellulose synthesis (BCS) membranes produced from treatments with various substrates after washing are shown in Fig. 1. The thickness of BCS is affected by nutritional elements such as polyphenols, which create optimal conditions for the growth of cellulose-producing bacteria. The membranes obtained from this process exhibited remarkable flexibility.

The production of SCOBY bacterial cellulose was influenced by the choice of fruit and vegetable media used. This variation stems from the diverse carbon sources present in the different raw materials, leading to disparities in BC quantity and SCOBY thickness. Furthermore, differences in water retention capabilities and structural characteristics affect both wet and dry weights, as well as overall productivity. The thickness of SCOBY is linked to fermentation duration and bacterial density, which in turn affects wet and dry weights. This is evidenced by studies showing that beet skin media yields 11.57 g/L, whereas glucose produces 13.07 g/L [69]. Additionally, mango skin waste hydrolysate significantly boosted BC yields from 0.52 g/L to 1.22 g/L through optimization [22]. Generally, a thicker SCOBY results in higher yields owing to increased biomass. Variations in SCOBY thickness can also influence the mechanical properties of the resulting cellulose, impacting its potential use [70]. Moreover, static fermentation affects the physical attributes of BC, leading to a more robust structure.

3.1. FE-SEM analysis of BCS

Surface morphology characteristics of Bacterial Cellulose from SCOBY (BCS) were scrutinized using Field-Emission Scanning Electron Microscopy (FE-SEM) at a magnification of 20,000× and 3.0 kV, as depicted in Fig. 2. The image illustrates that the membrane structure of BCS, generated across the five samples under investigation, showcases fine and densely packed cellulose fibers. Additionally, layers of cellulose intertwine, crisscross, and randomly stack, forming structures commonly recognized as micro fibrils.

Determining the distribution of micro fibril widths proves challenging due to the frequent twisting of cellulose ribbons by bacteria. This intricate network of cross-linked cellulose fibers exhibits diverse patterns and sizes. The BCS-KT (Fig. 2a) and BCS-NG (Fig. 2d) produced the largest average fiber diameter at 0.181 μm and 0.182 μm, respectively, followed by BCS-KL (Fig. 2b) and BCS-PS (Fig. 2e) at 0.110 μm and 0.111 μm. These BCS variants feature more pronounced pores, enhancing their water retention capacity.

Conversely, BCS-JB generated thinner or finer cellulose fibers, boasting an average size of 0.079 μm (Fig. 2c). This correlation between fiber diameter and polymer surface area influenced water vapor permeability. The findings aligned with the observations of [71,72], where thinner fibers contributed to increased surface area, imparting tensile strength and polymer elongation properties, resulting in a larger and porous hydrogel layer.

The size of cellulose fibers generated by SCOBY bacteria vary considerably depending on the nutritional sources used during fermentation, particularly fruits and vegetables. Specific biochemical pathways are activated by different carbon sources, which influence the production and structure of bacterial cellulose (BC). Wang et al. (2018) demonstrated that various carbon sources resulted in diverse BC characteristics, with fructose producing the highest yield [73]. A study by Ref. [74] revealed that industrial byproducts, such as beet molasses and vinasse, affect BC polymerization and crystallinity. Hasanin et al. (2023) observed that BC nanofibers derived from mango peel waste had a diameter of approximately 10 nm, while other sources yielded fibers of varying sizes [22]. Costa et al. (2017) found that BC produced from non-conventional media displayed improved thermal stability and crystallinity, which affected the fiber diameter and mechanical properties [75].

3.2. FTIR analysis

The outcomes from the Fourier Transform Infrared (FTIR) spectrum analysis of α-BCS, encompassing stretching and bending vibrations of different bonds, offered valuable insights into the chemical structure

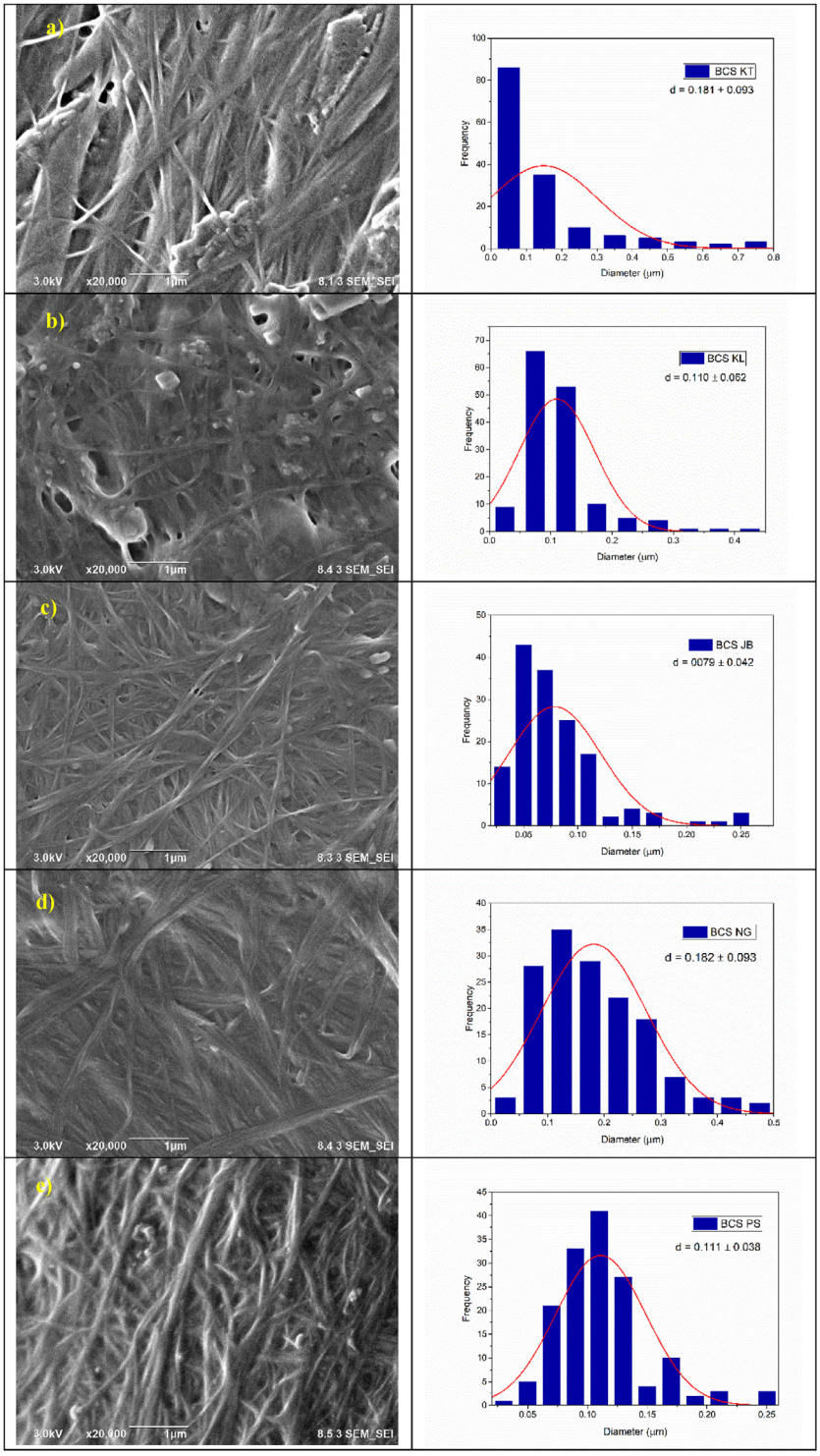

Fig. 2. FE-SEM analysis of bacterial cellulose from SCOBY (BCS) produced through fermentation of kombucha derived from fruits and vegetables.

and functionality of bacterial cellulose (Table 3). Fig. 3 illustrates the FTIR spectra produced by various media as byproducts of fermented beverages for the cultivation of α-BCS. The wavenumbers falling within the range of 3329.20–3338.12 cm^{-1}, situated in the 3200–3600 cm^{-1} range, signify O–H stretching, indicating the presence of O–H bonds in water molecules (H_2O) contained within α-BCS. This peak provided insights into the water content within the sample. In the sample, wavenumbers spanning

Table 3. FTIR peaks generated by α-BCS from fruit and vegetable byproducts.

Functional Group	Wavenumber (cm^{-1})					
	Std. α–Cellulose	α-BCS PS	α-BCS NG	α-BCS KT	α-BCS KL	α-BCS JB
O–H stretching	3329.20	3338.12	3338.22	3337.98	3336.96	3336.96
C–H stretching	2886.94	2893.85	2893.82	2891.34	2891.77	2892.95
O–H bending water H2O)	1639.63	1646.64	1643.81	1643.67	1643.65	1641.20
O–H bending (carboxylic acid)/ C–H bending	1427.61	1426.88	1427.53	1426.23	1426.08	1427.01
O–H bending (phenol)	1314.78	1313.90	1313.93	1313.63	1313.48	1313.89
C–O stretching (primary alcohol)	1156.93	1053.05	1053.71	1053.70	1052.78	1052.69
C–H bending (β-glicosidic)	897.16	900.04	899.49	900.01	899.95	899.31
C–H "out of plane bending"	662.23	662.39	663.92	663.56	663.01	661.08

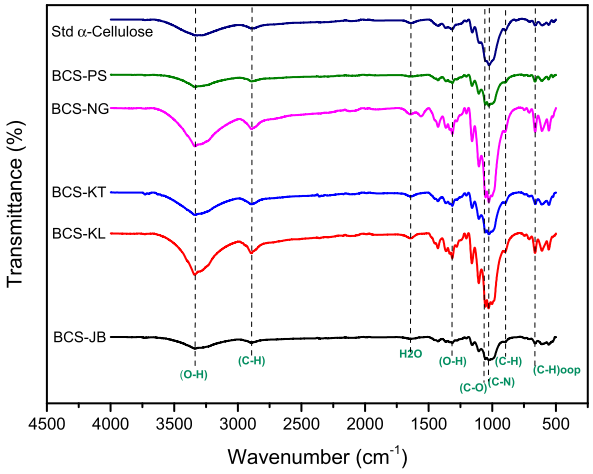

Fig. 3. FTIR spectra of the α-BCS kombucha byproduct from fruits and vegetables.

2886.94–2893.85 cm^{-1} represented C–H stretching vibrations associated with organic structures (C–H stretching). These peaks typically manifested across different frequency ranges, depending on the types of C–H bonds involved, signifying the presence of hydrocarbon groups in α-BCS.

Wavenumbers in the range of 1639.63–1646.64 cm^{-1} denoted O–H bending vibrations of water (H_2O) within the sample, appearing in the 1600–1800 cm^{-1} range. This implied the presence of O–H bond vibrations originating from water molecules (H_2O) and was linked to the water content in the sample. Within the range of 1426.88–1427.61 cm^{-1}, the bending vibrations of O–H in carboxylic acid groups or C–H bending vibrations of hydrocarbon groups were observed. The presence of this peak suggested the potential existence of carboxylic acid groups in α-BCS. This specific wavenumber range, 1420–1430 cm^{-1}, was also recognized as the crystallinity peak [76,77].

Wavenumbers spanning 1313.48–1314.78 cm^{-1} represent the bending vibrations of O–H linked to phenolic groups. The presence of this peak indicated the existence of phenolic groups in compounds within α-BCS. Wavenumbers between 1052.69 and 1156.93 cm^{-1} signified C–O stretching vibrations (primary alcohol), materializing within the 1000–1300 cm^{-1} frequency range. This suggested the possible presence of C–O bonds in primary alcohol groups within α-BCS. The absorption peak corresponding to the β-glycosidic cellulose bond (C–H bending) become evident at wavenumbers between 894.84 and 900.04 cm^{-1}, indicating the potential presence of C–H bonds involved in glycosidic bonds within α-BCS. This was also referred to as the amorphous absorption peak [78].

Finally, the wavenumbers falling within the range of 661.08–663.92 cm^{-1} signified "out of plane bending" C–H vibrations. This bending vibration encompassed various types of C–H bending vibrations occurring outside the molecular plane, indicative of the presence of C–H bonds in various orientations.

3.3. Analysis Liquid Holding Capacity (LHC)

Liquid Holding Capacity (LHC) denoted the ability of a material, specifically cellulose in this instance, to retain or absorb liquid. This quantification measured the volume of liquid that cellulose could absorb or retain under specific conditions. Despite cellulose's typically insoluble nature in most organic solvents owing to its crystalline structure [79], cellulose can exhibit swelling in certain solvents [55,80]. The depiction of α-BCS LHC is presented in Fig. 4.

The findings indicated a significant difference ($p < 0.05$). Among α-BCS-KT, α-BCS-PS, α-BCS-JB, and α-BCS-NG, DMSO's solvent absorption capacity allowed for the absorption of more liquid compared to water (H_2O). However, only α-BCS-KL demonstrated a greater ability to absorb water solvents than DMSO. This distinction may have been attributed to the heightened hydrophilicity of

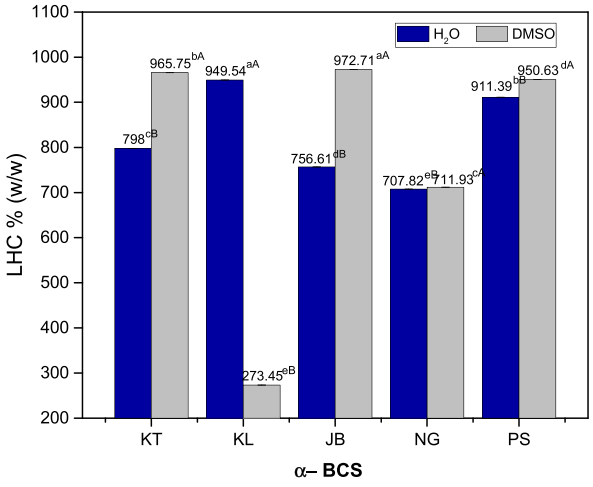

Fig. 4. LHC of the α-BCS kombucha byproduct from fruits and vegetables. Means indicated by distinct lowercase letters in the same color denote significant differences ($p < 0.05$), while means marked with different uppercase letters in various colors signify significant differences ($p < 0.05$).

α-cellulose in α-BCS-KL, suggesting a stronger affinity for water. In contrast, other α-BCS variants may have possessed specific structural or chemical characteristics in bacterial α-cellulose, making them more compatible with DMSO than water. DMSO exhibited greater polarity characteristics than other aprotic organic solvents, facilitating enhanced interaction with α-cellulose.

DMSO had the capability to disrupt strong hydrogen bonds, effectively intervening in the hydrogen bonds between α-cellulose molecules. This property allowed α-cellulose to retain more liquid in DMSO than in water. These observations were consistent with earlier research highlighting DMSO's high hydrogen bonding capacity [79,81] and the overall proficiency of all α-BCSs in retaining DMSO at a relatively higher rate than other liquids.

Liquid Holding Capacity (LHC) is of critical importance across various industries, including food, chemical, pharmaceutical, and textile sectors. In the food industry, LHC serves as a crucial metric for evaluating the capacity of materials, such as dietary fibers, to absorb water or fat, thereby influencing the texture and overall quality of food products [82,83]. In the textile sector, LHC plays a pivotal role in assessing the ability of fabrics or textile fibers to absorb perspiration and other fluids, directly impacting user comfort and experience [84–86]. Simultaneously, within the pharmaceutical industry, LHC emerges as a critical factor governing the controlled release of drugs from various dosage forms, profoundly affecting both the efficacy and safety of pharmaceutical products [87–89]. LHC stands as a pivotal parameter with far-reaching implications across diverse industries, playing a vital role in product design, quality assurance, and material performance.

3.4. XRD (X-ray diffraction) of α-BCS

XRD analysis serves the purpose of elucidating a material's crystal structure and X-ray diffraction pattern, particularly distinguishing between crystalline and amorphous structures. The data obtained from this analysis were instrumental in interpreting the crystallinity index and crystallite size of α-BCS. The degree of crystallinity is pivotal as it plays a crucial role in delineating the crystalline and amorphous regions within the molecules [90]. α-BCS derived from the byproducts of fruit and vegetable beverages exhibited three prominent peaks at 2θ angles. The X-ray diffraction pattern of α-BCS, produced by media KT, KL, JB, NG, PS, and standard α-cellulose, is visually represented in Fig. 5. These three significant peaks d1 (101 = 14.4°), d2 (10i = 16.6°), and d3 (002 = 22.5°) were prevalent in the products from all five media, signifying the cellulose type I (Table 4). Cellulose Iα was characterized by parallel chains that interact through intermolecular hydrogen bonds, stabilized by van der Waals interactions [91]. Within this context, the crystallinity index (CI) is defined as the ratio of crystalline regions to the overall polymer structure, accounting for both crystalline and amorphous regions.

Among the three crystalline peaks, the highest peak (002) was considered for calculations, as it was the primary indicator of cellulose crystallinity [92]. These three peaks were recognized as the characteristic peaks for cellulose. The crystallinity index is computed based on the peak intensity data, utilizing the Segal method [52,53]. The minimum position between peaks 002 and 101, denoted as I_{AM} (located around 18.3° in Fig. 5), represented a peak that was not parallel to the maximum height of the amorphous peak. Peaks originating from amorphous cellulose were likely to have values higher than 18.3°.

The crystallinity index of BCS derived from the five alternative media did not exhibit significant differences. However, the CI values for α-BCS across all five media surpassed 90%, in contrast to the standard α-cellulose (77.50%). Although α-BCS-JB achieved the highest crystallinity index, it did not significantly differ from α-BCS-KL and α-BCS-NG, each displaying values of 93.87%, 93.50%, and 93.12%, respectively. α-BCS-PS and α-BCS-KT followed closely with values of 91.75% and 91.62%. The

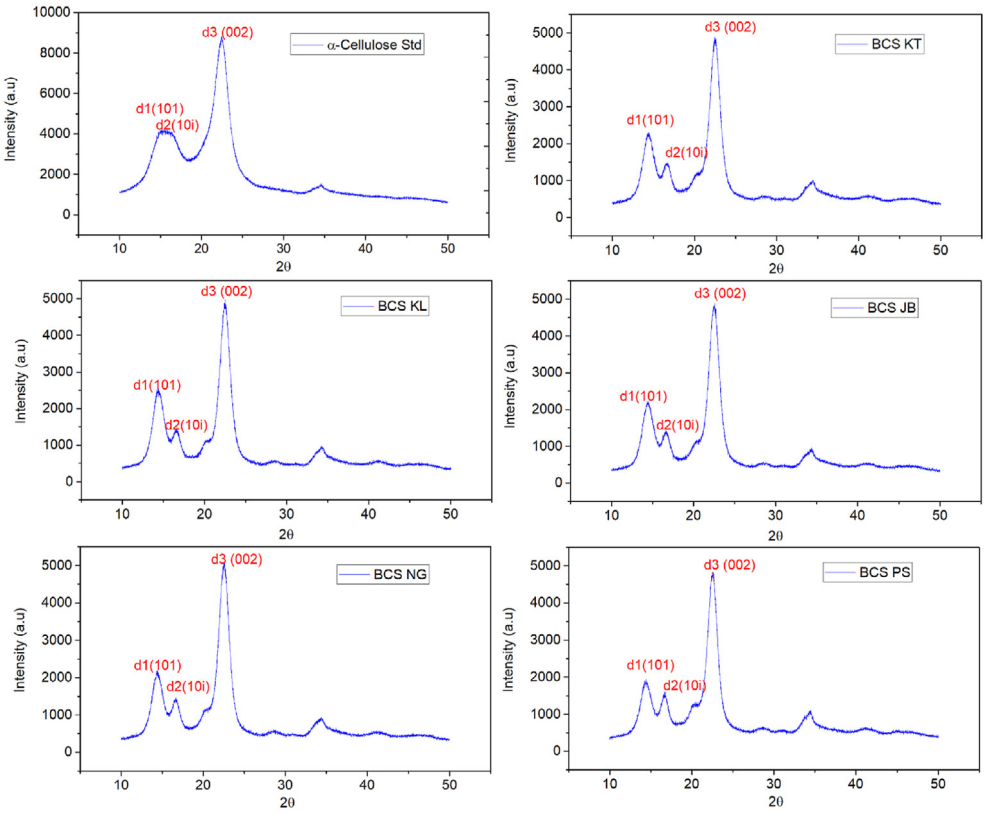

Fig. 5. XRD of the α-BCS kombucha byproduct from fruits and vegetables.

X-ray diffraction peak intensity on the (002) crystal plane (2θ = 22.5) was more pronounced than on the (101) (2θ = 14.3) and (10i) (2θ = 16.6) crystal planes in the α-BCS products.

Various factors impact Bacterial cellulose (BC) crystallinity, including culture method, carbon source, pH, agitation speed, temperature, fermentation time, and drying method [55]. Additionally,

Table 4. Three main peak positions (2θ), Full width at half maximum (FWHM), the crystallite size (CrS) and crystallinity index (CI) of the α-BCS kombucha byproduct from fruits and vegetables.

Medium	*(Crstaline peak)*	Peak position (2θ)	FWHM[a] (2θ)	CrS[b] (nm)	CI (%)
Std. Alpha cellulose	d1 (101)	14.94	1.28	6.54	77.50
	d2 (10i)	16.70	2.30	3.65	
	d3 (002)	22.42	2.55	3.32	
KT	d1 (101)	14.44	1.75	4.78	91.62
	d2 (10i)	16.69	1.00	8.40	
	d3 (002)	22.54	1.51	5.61	
KL	d1 (101)	14.39	1.68	4.99	93.50
	d2 (10i)	16.55	1.20	7.01	
	d3 (002)	22.51	1.47	5.77	
JB	d1 (101)	14.39	1.69	4.95	93.87
	d2 (10i)	16.62	1.29	6.52	
	d3 (002)	22.53	1.42	5.94	
NG	d1 (101)	14.40	1.65	5.07	93.12
	d2 (10i)	16.65	1.14	7.36	
	d3 (002)	22.53	1.48	5.73	
PS	d1 (101)	14.40	1.66	5.04	91.75
	d2 (10i)	16.66	1.15	7.27	
	d3 (002)	22.53	1.33	6.35	

[a] Measured at half of the max intensity height.
[b] Calculated using the Debye Scherrer equation based on the XRD diffraction pattern.

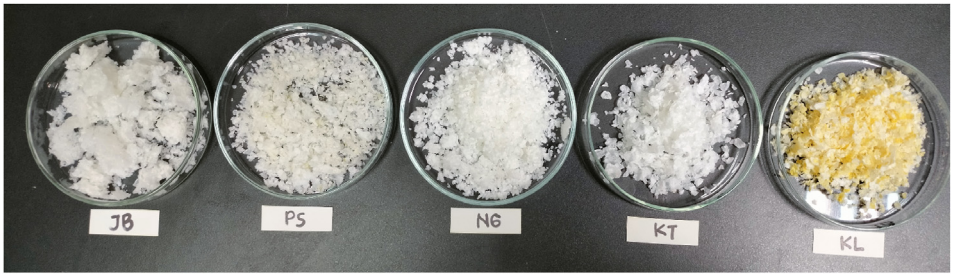

Fig. 6. The α-BCS derived from byproducts of Kombucha from fruits and vegetables.

the type of fermentation media, nutrient parameters, and drying methods play a pivotal role in determining the crystallinity ratio of BCs [93]. Prior studies have highlighted how the crystallinity of BCs produced with different microorganism strains and carbon sources also influences crystallinity, with media contributing to cellulose production [94]. Furthermore, crystallinity is vital in determining the mechanical properties of any macromolecule. In this study, the choice of media significantly influenced the crystallinity of the resulting α-BCS. The byproducts from fruit and vegetable fermentation exhibit unique characteristics, offering potential applications in the food, pharmaceutical, and packaging industries. This opens avenues for product innovation and diversification, highlighting the versatility of these byproducts in developing valuable materials for various industrial sectors.

The crystal size was calculated using equation (5), which was based on the wavelength, full width at half maximum (FWHM), and 2θ values extracted from the XRD test results on the cellulose samples produced. Table 4 provides details on the crystallite size (CrS) and full width at half maximum (FWHM) of α-BCS from various sources. The results indicated that the crystallite size ranged from 4.78 to 8.40 nm, surpassing the standard α-cellulose. These values underscored the effectiveness of alkali hydrolysis treatment in eliminating the amorphous component of cellulose. Alteration in the XRD pattern at the characteristic cellulose peaks signified alterations in crystallinity index and crystal size, as evidenced by the sharper peak intensity values.

Crystal size refers to the dimensions of crystalline particles within the cellulose material. A larger crystal size implies larger crystalline particles, reflecting the level of regularity in crystal arrangement, as manifested by the width of the peak in the XRD spectrum (FWHM). A narrower peak signifies a more uniform distribution of crystal sizes and a higher degree of crystallinity. Conversely, a broader peak indicates a wider distribution of crystal sizes, potentially corresponding to lower crystallinity. A narrower FWHM implies a more homogeneous distribution of crystal sizes and a higher degree of crystallinity [95]. Fig. 6 visually illustrates the isolation of α-cellulose from the produced BCS samples.

4. Conclusion

In conclusion, this research successfully achieved the production of Bacterial Cellulose from fermented beverage byproducts using kombucha SCOBY (BCS) with diverse vegetable and fruit substrates. This research demonstrates that bacterial cellulose from SCOBY (BCS) production from fermented beverage substrates results in BCS with distinct chemical and morphological characteristics during the fermentation process, depending on the specific substrate. Notably, total reducing sugars (TRS) decreased, protein levels remained relatively stable, and phenolic content increased. Fluctuations were observed in flavonoid levels and antioxidant activity throughout fermentation. Additionally, the thickness and moisture content of BCS varied across fermentation substrate media, and morphological analysis showcased differences in cellulose fiber size. FTIR analysis identified distinct functional groups in α-BCS, reflecting the presence of C−H stretching bonds, O−H bending, C−H_2 bending, C−O stretching, and C−H bending (β-glycosidic). XRD results demonstrated that all α-BCS substrates, derived from both vegetable and fruit substrates, exhibited a high crystallinity index (CrI >90%), with α-BCS-JB having the highest crystallinity index among the substrates. This study provides valuable insights into the production of α-BCS from alternative sources, offering a comprehensive understanding of its chemical and morphological properties. The implications of these findings extend to diverse fields, including food, pharmaceuticals, biomedicine, and composite materials. The successful production of BCS from varied substrates presents opportunities for novel applications and sustainable practices in material science and biotechnology. Multiple biological and pharmaceutical properties are essential to establish guidelines for BCS applications.

Funding

This work was supported by the National Agency for Research and Innovation, Indonesia with contract No. 20/III.10/HK/2024.

Ethics information

This research does not involve ethical concerns, as it does not utilize test animals.

Acknowledgements

Financial guarantee was supported by the Molecular Fundamental Science Program's and the Nanotechnology and Advanced Materials Program's, the National Agency for Research and Innovation, Indonesia. The authors acknowledge the facilities, scientific and technical support from Advanced Characterization Laboratories Serpong, National Research and Innovation Institute through E-Layanan Sains, Badan Riset dan Inovasi Nasional, Indonesia.

Abbreviations and glossary

BC	Bacterial Cellulose
BCS	Bacterial Cellulose from SCOBY
α-BCS	alpha - Bacterial Cellulose from SCOBY
SCOBY	Symbiotic culture of bacteria and yeast
CMC	Carboxymethyl cellulose
HEC	Hydroxyethyl cellulose
KT	*Katuk* leaves
KL	*Kale* leaves
JB	Guava
NG	Dragon fruit
PS	Banana
DNS	3, 5-dinitrosalicylic acid
TRS	Total Reducing Sugar
DPPH	2,2-diphenyl-1-picryl-hydrazyl-hydrate
FE-SEM	Field-Emission Scanning Electron Microscope
NaOH	Sodium hydroxide
XRD	X-Ray Diffraction
ATR	Attenuated total reflection
FTIR	Fourier-transform infrared
CI	Crystallinity Index
I_{002}	Intensity of the crystalline region at 2θ (≈22.5°)
IAM	Intensity of the amorphous region at 2θ (≈18.3°)
CrS	Crystallite size
(k)	constant (dimensionless Scherrer constant, which equals 0.9)
(λ)	lambda (wavelength of X-ray diffraction)
FWHM	full width at half maximum in radians
(Θ)	theta (the diffraction angle in radians)
LHC	Liquid holding capacity
DMSO	Dimethyl sulfoxide
H_2O	Hydrogen oxide (water)
ΔpH	delta pH (change in potential of Hydrogen referred to as acidity or basicity)
d	means of diameter fibers
2θ	twotheta (2 θ is the angle between transmitted beam and reflected beam)
d1, d2, d3	crystalline peaks (101, 10$\bar{1}$, 002)

References

[1] C.E.M. Aydemir, S. Yenidoğan, D. Tutak, Sustainability in the print and packaging industry, Cellul Chem Technol 57 (2023) 565–577, https://doi.org/10.35812/cellulosechemtechnol.2023.57.51.

[2] R.A. Sheldon, D. Brady, Green chemistry, biocatalysis, and the chemical industry of the future, Chem Sus Chem 15 (2022) e202102628, https://doi.org/10.1002/cssc.202102628.

[3] N.H. Avcioglu, Bacterial cellulose: recent progress in production and industrial applications, World J Microbiol Biotechnol 38 (2022) 86, https://doi.org/10.1007/s11274-022-03271-y.

[4] S. Manan, M.W. Ullah, M. Ul-Islam, Z. Shi, M. Gauthier, G. Yang, Bacterial cellulose: molecular regulation of biosynthesis, supramolecular assembly, and tailored structural and functional properties, Prog Mater Sci 129 (2022) 100972, https://doi.org/10.1016/j.pmatsci.2022.100972.

[5] B. Behera, D. Laavanya, P. Balasubramanian, Techno-economic feasibility assessment of bacterial cellulose biofilm production during the Kombucha fermentation process, Bioresour Technol 346 (2022) 126659, https://doi.org/10.1016/j.biortech.2021.126659.

[6] Y.A.R. Tapias, M.V. Di Monte, M.A. Peltzer, A.G. Salvay, Bacterial cellulose films production by kombucha symbiotic community cultured on different herbal infusions, Food Chem 372 (2022) 131346, https://doi.org/10.1016/j.foodchem.2021.131346.

[7] S.S. Muthu, R. Rathinamoorthy, Bacterial Cellulose: Sustainable Material for Textiles, Springer Nature. 2021, https://doi.org/10.1007/978-981-15-9581-3.

[8] B. V Mohite, S. V Patil, A novel biomaterial: bacterial cellulose and its new era applications, Biotechnol Appl Biochem 61 (2014) 101–110, https://doi.org/10.1002/bab.1148.

[9] A.L.V. Cubas, A.P. Provin, A.R.A. Dutra, C. Mouro, I.C. Gouveia, Advances in the production of biomaterials through kombucha using food waste: concepts, challenges, and potential, Polymers 15 (2023) 1701, https://doi.org/10.3390/polym15071701.

[10] H. Antolak, D. Piechota, A. Kucharska, Kombucha tea—a double power of bioactive compounds from tea and symbiotic culture of bacteria and yeasts (SCOBY), Antioxidants 10 (2021) 1541, https://doi.org/10.3390/antiox10101541.

[11] J. Martínez Leal, L. Valenzuela Suárez, R. Jayabalan, J. Huerta Oros, A. Escalante-Aburto, A review on health benefits of kombucha nutritional compounds and metabolites, CyTA J Food 16 (2018) 390–399, https://doi.org/10.1080/19476337.2017.1410499.

[12] R.M.D. Coelho, A.L. de Almeida, R.Q.G. do Amaral, R.N. da Mota, P.H.M. de Sousa, Kombucha, Int J Gastron Food Sci 22 (2020) 100272, https://doi.org/10.1016/j.ijgfs.2020.100272.

[13] M.E. Pacheco-Montealegre, L.L. Dávila-Mora, L.M. Botero-Rute, A. Reyes, A. Caro-Quintero, Fine resolution analysis of microbial communities provides insights into the variability of cocoa bean fermentation, Front Microbiol 11 (2020) 650, https://doi.org/10.3389/fmicb.2020.00650.

[14] D.A. Hamed, H.H. Maghrawy, H. Abdel Kareem, Biosynthesis of bacterial cellulose nanofibrils in black tea media by a symbiotic culture of bacteria and yeast isolated from commercial kombucha beverage, World J Microbiol Biotechnol. 39 (2023) 48, https://doi.org/10.1007/s11274-022-03485-0.

[15] V. Potočnik, S. Gorgieva, J. Trček, From nature to lab: sustainable bacterial cellulose production and modification with synthetic biology, Polymers 15 (2023) 3466, https://doi.org/10.3390/polym15163466.

[16] K.R. Harrison, Elucidating the patterns of cooccurrence, spatial structuring, and impact on fermentation metabolism in kombucha microbial communities. Doctoral Dissertation, Oregon State University. 2023.

[17] S.A. Villarreal-soto, S. Beaufort, J. Bouajila, J. Souchard, P. Taillandier, Understanding kombucha tea fermentation,

A review 83 (2018) 575–873, https://doi.org/10.1111/1750-3841.14068.
[18] N.N. Yassunaka Hata, M. Surek, D. Sartori, R. Vassoler Serrato, W. Aparecida Spinosa, Role of acetic acid bacteria in food and beverages, Food Technol Biotechnol 61 (2023) 85–103, https://doi.org/10.17113/ftb.61.01.23.7811.
[19] M.A. Bryszewska, E. Tabandeh, J. Jędrasik, M. Czarnecka, J. Dzierżanowska, K. Ludwicka, SCOBY cellulose modified with apple powder—biomaterial with functional characteristics, Int J Mol Sci 24 (2023) 1005, https://doi.org/10.3390/ijms24021005.
[20] P. Jittaut, P. Hongsachart, S. Audtarat, T. Dasri, Production and characterization of bacterial cellulose produced by *Gluconacetobacter xylinus* BNKC 19 using agricultural waste products as nutrient source, Arab J Basic Appl Sci 30 (2023) 221–230, https://doi.org/10.1080/25765299.2023.2172844.
[21] M. Ramírez-Carmona, M.P. Gálvez-Gómez, L. González-Perez, V. Pinedo-Rangel, T. Pineda-Vasquez, D. Hotza, Production of bacterial cellulose hydrogel and its evaluation as a proton exchange membrane, J Polym Environ 31 (2023) 2462–2472, https://doi.org/10.1007/s10924-023-02759-4.
[22] M.S. Hasanin, M. Abdelraof, A.H. Hashem, H. El Saied, Sustainable bacterial cellulose production by *Achromobacter* using mango peel waste, Microb Cell Factories 22 (2023) 24, https://doi.org/10.1186/s12934-023-02031-3.
[23] U. Sarker, M.N. Hossain, M.A. Iqbal, S. Oba, Bioactive components and radical scavenging activity in selected advance lines of salt-tolerant vegetable amaranth, Front Nutr 7 (2020) 587257, https://doi.org/10.3389/fnut.2020.587257.
[24] M.M. Rahaman, R. Hossain, J. Herrera-Bravo, M.T. Islam, O. Atolani, O.S. Adeyemi, O.A. Owolodun, L. Kambizi, S.D. Daştan, D. Calina, Natural antioxidants from some fruits, seeds, foods, natural products, and associated health benefits: an update, Food Sci Nutr 11 (2023) 1657–1670, https://doi.org/10.1002/fsn3.3217.
[25] S. Maheshwari, V. Kumar, G. Bhadauria, A. Mishra, Immunomodulatory potential of phytochemicals and other bioactive compounds of fruits: a review, Food Front 3 (2022) 221–238, https://doi.org/10.1002/fft2.129.
[26] N. Kozyrovska, O. Reva, O. Podolich, O. Kukharenko, I. Orlovska, V. Terzova, G. Zubova, A.P. Trovatti Uetanabaro, A. Góes-Neto, V. Azevedo, To other planets with upgraded millennial kombucha in rhythms of sustainability and health support, Front Astron Sp Sci 8 (2021) 701158, https://doi.org/10.3389/fspas.2021.701158.
[27] S. Charoenrak, S. Charumanee, P. Sirisa-Ard, S. Bovonsombut, L. Kumdhitiahutsawakul, S. Kiatkarun, W. Pathom-Aree, T. Chitov, S. Bovonsombut, Nanobacterial cellulose from kombucha fermentation as a potential protective carrier of *Lactobacillus plantarum* under simulated gastrointestinal tract conditions, Polymers 15 (2023) 1356, https://doi.org/10.3390/polym15061356.
[28] M. Abdelraof, M.S. Hasanin, H. El-Saied, Ecofriendly green conversion of potato peel wastes to high productivity bacterial cellulose, Carbohydr Polym 211 (2019) 75–83, https://doi.org/10.1016/j.carbpol.2019.01.095.
[29] M. Salari, M.S. Khiabani, R.R. Mokarram, B. Ghanbarzadeh, H.S. Kafil, Preparation and characterization of cellulose nanocrystals from bacterial cellulose produced in sugar beet molasses and cheese whey media, Int J Biol Macromol 122 (2019) 280–288, https://doi.org/10.1016/j.ijbiomac.2018.10.136.
[30] A. Kadier, R.A. Ilyas, M.R.M. Huzaifah, N. Harihastuti, S.M. Sapuan, M.M. Harussani, M.N.M. Azlin, R. Yuliasni, R. Ibrahim, M.S.N. Atikah, Use of industrial wastes as sustainable nutrient sources for bacterial cellulose (BC) production: mechanism, advances, and future perspectives, Polymers 13 (2021) 3365, https://doi.org/10.3390/polym13193365.
[31] H. El-Gendi, T.H. Taha, J.B. Ray, A.K. Saleh, Recent advances in bacterial cellulose: a low-cost effective production media, optimization strategies and applications, Cellulose 29 (2022) 7495–7533, https://doi.org/10.1007/s10570-022-04697-1.
[32] R. Sharma, H.S. Oberoi, G.S. Dhillon, Fruit and vegetable processing waste: renewable feed stocks for enzyme production, in: G.S. Dhillon, S. Kaur, eds., Agro-Industrial Wastes as Feed. Enzym. Prod, Academic Press Elsevier. 2016, pp. 23–59, https://doi.org/10.1016/B978-0-12-802392-1.00002-2.
[33] S. Shrestha, J.R. Khatiwada, H.K. Sharma, W. Qin, Bioconversion of fruits and vegetables wastes into value-added products, Sustain Bioconversion Waste to Value Added Prod (2021) 145–163, https://doi.org/10.1007/978-3-030-61837-7_9.
[34] C. Ipsit, Fruit and vegetable waste utilization and sustainability, in: S.A. Mandavgane, I. Chakravarty, A.K. Jaiswal, eds., Fruit and Vegetable Waste Utilization and Sustainability, Academic Press Elsevier. 2023, pp. 1–18, https://doi.org/10.1016/B978-0-323-91743-8.00009-5.
[35] Y. Maryati, H. Melanie, A. Susilowati, E. Filailla, H. Mulyani, A. Aspiyanto, S. Budiari, N. Artanti, A.F. Devi, W. Handayani, Y. Yasman, Optimization of process conditions for fermented banana using SCOBY in producing bioactive compounds and antioxidant activity by CCD-RSM design, AIP Conf Proc 2902 (2023) 060018, https://doi.org/10.1063/5.0173156.
[36] Y. Maryati, A. Susilowati, H. Mulyani, E. Filailla, H. Melanie, S. Budiari, A. Aspiyanto, W. Handayani, Y. Yasman, Changes in total phenolic concentration and antioxidant capacity of fermented guava (Psidium guajava) juice extract by SCOBY, AIP Conf Proc 2972 (2023) 050009, https://doi.org/10.1063/5.0186804.
[37] H. Mulyani, N. Artanti, E. Filailla, S. Budiari, Y. Maryati, H. Melanie, A. Susilowati, R. Yuniati, Y. Yasman, Effect of fermented red ginger (Zingiber officinale var. rubrum) using kombucha culture toward free radical scavenging activity, AIP Conf Proc 2902 (2023) 060022, https://doi.org/10.1063/5.0173149.
[38] K. Harrison, C. Curtin, Microbial composition of SCOBY starter cultures used by commercial kombucha brewers in North America, Microorganisms 9 (2021) 1060, https://doi.org/10.3390/microorganisms9051060.
[39] S. Reyes-Flores, T.S.S. Pereira, M.M. Ramírez-Rodrigues, Optimization of hempseed-added kombucha for increasing the antioxidant capacity, protein concentration, and total phenolic content, Beverages 9 (2023) 50, https://doi.org/10.3390/beverages9020050.
[40] S. Saher, H. Saleem, A.M. Asim, M. Uroos, N. Muhammad, Pyridinium based ionic liquid: a pretreatment solvent and reaction medium for catalytic conversion of cellulose to total reducing sugars (TRS), J Mol Liq 272 (2018) 330–336, https://doi.org/10.1016/j.molliq.2018.09.099.
[41] A.D. Abdullahi, P. Kodchasee, K. Unban, T. Pattananandecha, C. Saenjum, A. Kanpiengjai, K. Shetty, C. Khanongnuch, Comparison of phenolic contents and scavenging activities of miang extracts derived from filamentous and non-filamentous fungi-based fermentation processes, Antioxidants 10 (2021) 1144, https://doi.org/10.3390/antiox10071144.
[42] B.E. Tefon Öztürk, B. Eroğlu, E. Delik, M. Çiçek, E. Çiçek, Comprehensive evaluation of three important herbs for kombucha fermentation, Food Technol Biotechnol 61 (2023) 127–137, https://doi.org/10.17113/ftb.61.01.23.7789.
[43] B.M. Vohra, S. Fazry, F. Sairi, O. Babul-Airianah, Effects of medium variation and fermentation time on the antioxidant and antimicrobial properties of kombucha, Malaysian J Fundam Appl Sci 15 (2019) 298–302, https://doi.org/10.11113/mjfas.v15n2-1.1536.
[44] F. Sederavičiūtė, P. Bekampienė, J. Domskienė, Effect of pretreatment procedure on properties of kombucha fermented bacterial cellulose membrane, Polym Test 78 (2019) 105941, https://doi.org/10.1016/j.polymertesting.2019.105941.
[45] Y.F. Cavalcanti, J.D. Amorim, A.D. Medeiros, C.J.G. da Silva Jr., I.J. Durval, A.F. Costa, L.A. Sarubbo, Microbial cellulose production with tomato (*Solanum lycopersicum*) residue for industrial applications, Chem Eng Trans 100 (2023) 409–414, https://doi.org/10.3303/CET23100069.

[46] D. Abol-Fotouh, M.A. Hassan, H. Shokry, A. Roig, M.S. Azab, A.E.-H.B. Kashyout, Bacterial nanocellulose from agro-industrial wastes: low-cost and enhanced production by *Komagataeibacter saccharivorans* MD1, Sci Rep 10 (2020) 3491, https://doi.org/10.1038/s41598-020-60315-9.
[47] H. Kaur, B. Rana, D. Tomar, S. Kaur, K.C. Jena, Fundamentals of ATR-FTIR spectroscopy and its role for probing in-situ molecular-level interactions, Progress in Optic Sci and Photonics 13 (2021) 3–37, https://doi.org/10.1007/978-981-33-6084-6_1.
[48] R. Janus, M. Wądrzyk, M. Lewandowski, K. Zaborowska, Ł. Korzeniowski, M. Plata, A novel capillary forces-founded accessory for reliable measurements of ATR-FTIR spectra of volatile liquids, Microchem J 185 (2023) 108219, https://doi.org/10.1016/j.microc.2022.108219.
[49] R. Muttaqin, Pengembangan buku panduan teknik karakterisasi material: X-ray diffractometer (XRD) panalytical Xpert3 powder, Indones J Lab 1 (n.d.) 9–16. https://doi.org/10.22146/ijl.v1i1.78970.
[50] L.A. Didik, Penentuan ukuran butir kristal CuCr0,98-Ni0,02O2 dengan menggunakan x-ray difraction (XRD) dan scanning electron microscope (SEM), Indones, Phys Rev 3 (2020) 6–14, https://doi.org/10.29303/ipr.v3i1.37.
[51] L. Segal, J.J. Creely, A.E. Martin Jr., C.M. Conrad, An empirical method for estimating the degree of crystallinity of native cellulose using the X-ray diffractometer, Textil Res J 29 (1959) 786–794, https://doi.org/10.1177/004051755902901003.
[52] S. Park, J.O. Baker, M.E. Himmel, P.A. Parilla, D.K. Johnson, Cellulose crystallinity index: measurement techniques and their impact on interpreting cellulase performance, Biotechnol Biofuels 3 (2010) 1–10, https://doi.org/10.1186/1754-6834-3-10.
[53] S. Nam, A.D. French, B.D. Condon, M. Concha, Segal crystallinity index revisited by the simulation of X-ray diffraction patterns of cotton cellulose Iβ and cellulose II, Carbohydr Polym 135 (2016) 1–9, https://doi.org/10.1016/j.carbpol.2015.08.035.
[54] S.-C. Wu, M.-H. Li, Production of bacterial cellulose membranes in a modified airlift bioreactor by Gluconacetobacter xylinus, J Biosci Bioeng 120 (2015) 444–449, https://doi.org/10.1016/j.jbiosc.2015.02.018.
[55] M. Güzel, Ö. Akpõnar, Production and characterization of bacterial cellulose from citrus peels, Waste and Biomass Valorization 10 (2019) 2165–2175, https://doi.org/10.1007/s12649-018-0241-x.
[56] R.R. Elfirta, P.R. Ferdian, I. Saskiawan, T.H. Handayani, K.F. G. Mandalika, R. Riffiani, K. Kasirah, U.M.S. Purwanto, Antioxidant properties of kombucha beverage infused with *Ganoderma lucidum* and green tea from *Camellia sinensis* (L.) Kuntze with several fermentation times, Karbala Int J Mod Sci 10 (2024) 141–152, https://doi.org/10.33640/2405-609X.3345.
[57] A. Sknepnek, S. Tomić, D. Miletić, S. Lević, M. Čolić, V. Nedović, M. Nikšić, Fermentation characteristics of novel *Coriolus versicolor* and *Lentinus edodes* kombucha beverages and immunomodulatory potential of their polysaccharide extracts, Food Chem 342 (2021) 128344, https://doi.org/10.1016/j.foodchem.2020.128344.
[58] F. Yassine, N. Bassil, R. Flouty, A. Chokr, A. El Samrani, G. Boiteux, M. El Tahchi, Culture medium pH influence on Gluconacetobacter physiology: cellulose production rate and yield enhancement in presence of multiple carbon sources, Carbohydr Polym 146 (2016) 282–291, https://doi.org/10.1016/j.carbpol.2016.02.003.
[59] Y. Mengesha, A. Tebeje, B. Tilahun, A review on factors influencing the fermentation process of Teff (Eragrostis teff) and other cereal-based Ethiopian injera, Int J Food Sci 2022 (2022) 10, https://doi.org/10.1155/2022/4419955, 4419955.
[60] T.M. Tirtawinata, Optimization of kombucha production flow and hygienity, research on scaling-up production, and stabilizing kombucha, I3L Sci Repos (2023) 1–27. http://repository.i3l.ac.id/jspui/handle/123456789/672.
[61] B.K. Vargas, M.F. Fabricio, M.A.Z. Ayub, Health effects and probiotic and prebiotic potential of kombucha: a bibliometric and systematic review, Food Biosci 44 (2021) 101332, https://doi.org/10.1016/j.fbio.2021.101332.
[62] K. Jakubczyk, J. Kałduńska, J. Kochman, K. Janda, Chemical profile and antioxidant activity of the kombucha beverage derived from white, green, black and red tea, Antioxidants 9 (2020) 447, https://doi.org/10.3390/antiox9050447.
[63] D.R. Lopes, L.O. Santos, C. Prentice-Hernández, Antioxidant and antibacterial activity of a beverage obtained by fermentation of yerba-maté (*Ilex paraguariensis*) with symbiotic kombucha culture, J Food Process Preserv 45 (2021) e15101, https://doi.org/10.1111/jfpp.15101.
[64] N.-Ł. Zofia, Z. Aleksandra, B. Tomasz, Z.-D. Martyna, Z. Magdalena, H.-B. Zofia, W. Tomasz, Effect of fermentation time on antioxidant and anti-ageing properties of green coffee kombucha ferments, Molecules 25 (2020) 5394, https://doi.org/10.3390/molecules25225394.
[65] N. Folmann Lima, G.M. Maciel, I. de Andrade Arruda Fernandes, C. Windson Isidoro Haminiuk, Optimising the production process of bacterial nanocellulose: impact on growth and bioactive compounds, Food Technol Biotechnol 61 (2023) 494–504, https://doi.org/10.17113/ftb.61.04.23.8182.
[66] H. Kim, S. Hur, J. Lim, K. Jin, T. Yang, I. Keehm, S.W. Kim, T. Kim, D. Kim, Enhancement of the phenolic compounds and antioxidant activities of kombucha prepared using specific bacterial and yeast, Food Biosci 56 (2023) 103431, https://doi.org/10.1016/j.fbio.2023.103431.
[67] S. Zhang, S. Winestrand, X. Guo, L. Chen, F. Hong, L.J. Jönsson, Effects of aromatic compounds on the production of bacterial nanocellulose by *Gluconacetobacter xylinus*, Microb Cell Factories 13 (2014) 1–11, https://doi.org/10.1186/1475-2859-13-62.
[68] R. Malbaša, E. Lončar, M. Djurić, I. Došenović, Effect of sucrose concentration on the products of kombucha fermentation on molasses, Food Chem 108 (2008) 926–932, https://doi.org/10.1016/j.foodchem.2007.11.069.
[69] S. Beluhan, F. Herceg, A. Leboš Pavunc, S. Djaković, Preparation and structural properties of bacterial nanocellulose obtained from beetroot peel medium, Energies 15 (2022) 9374, https://doi.org/10.3390/en15249374.
[70] G. Sperotto, L.G. Stasiak, J.P.M.G. Godoi, N.C. Gabiatti, S.S. De Souza, A review of culture media for bacterial cellulose production: complex, chemically defined and minimal media modulations, Cellulose 28 (2021) 2649–2673, https://doi.org/10.1007/s10570-021-03754-5.
[71] N. Grishkewich, N. Mohammed, J. Tang, K.C. Tam, Recent advances in the application of cellulose nanocrystals, Curr Opin Colloid Interface Sci 29 (2017) 32–45, https://doi.org/10.1016/j.cocis.2017.01.005.
[72] D.A. Gregory, L. Tripathi, A.T.R. Fricker, E. Asare, I. Orlando, V. Raghavendran, I. Roy, Bacterial cellulose: a smart biomaterial with diverse applications, Mater Sci Eng R Rep 145 (2021) 100623, https://doi.org/10.1016/j.mser.2021.100623.
[73] S.-S. Wang, Y.-H. Han, J.-L. Chen, D.-C. Zhang, X.-X. Shi, Y.-X. Ye, D.-L. Chen, M. Li, Insights into bacterial cellulose biosynthesis from different carbon sources and the associated biochemical transformation pathways in *Komagataeibacter* sp, W1, Polymers (Basel) 10 (2018) 963, https://doi.org/10.3390/polym10090963.
[74] R.L. Heydorn, D. Lammers, M. Gottschling, K. Dohnt, Effect of food industry by-products on bacterial cellulose production and its structural properties, Cellulose 30 (2023) 4159–4179, https://doi.org/10.1007/s10570-023-05097-9.
[75] A.F.S. Costa, F.C.G. Almeida, G.M. Vinhas, L.A. Sarubbo, Production of bacterial cellulose by *Gluconacetobacter hansenii* using corn steep liquor as nutrient sources, Front Microbiol 8 (2017) 2027, https://doi.org/10.3389/fmicb.2017.02027.
[76] V. Hospodarova, E. Singovszka, N. Stevulova, Characterization of cellulosic fibers by FTIR spectroscopy for their further

implementation to building materials, Am J Anal Chem 9 (2018) 303–310, https://doi.org/10.4236/ajac.2018.96023.
[77] R. Vârban, I. Crișan, D. Vârban, A. Ona, L. Olar, A. Stoie, R. Ștefan, Comparative FT-IR prospecting for cellulose in stems of some fiber plants: flax, velvet leaf, hemp and jute, Appl Sci 11 (2021) 8570, https://doi.org/10.3390/app11188570.
[78] S. Gorgieva, U. Jančič, E. Cepec, J. Trček, Production efficiency and properties of bacterial cellulose membranes in a novel grape pomace hydrolysate by *Komagataeibacter melomenusus* AV436^T and *Komagataeibacter xylinus* LMG 1518, Int J Biol Macromol 244 (2023) 125368, https://doi.org/10.1016/j.ijbiomac.2023.125368.
[79] W.N. Goh, A. Rosma, B. Kaur, A. Fazilah, A.A. Karim, R. Bhat, Microstructure and physical properties of microbial cellulose produced during fermentation of black tea broth (Kombucha). II, Int Food Res J 19 (2012) 153–158.
[80] G.I. Mantanis, R.A. Young, R.M. Rowell, Swelling of compressed cellulose fiber webs in organic liquids, Cellulose 2 (1995) 1–22, https://doi.org/10.1007/BF00812768.
[81] M. Güzel, Ö. Akpõnar, Preparation and characterization of bacterial cellulose produced from fruit and vegetable peels by *Komagataeibacter hansenii* GA2016, Int J Biol Macromol 162 (2020) 1597–1604, https://doi.org/10.1016/j.ijbiomac.2020.08.049.
[82] V. Tejada-Ortigoza, L.E. Garcia-Amezquita, S.O. Serna-Saldívar, J. Welti-Chanes, Advances in the functional characterization and extraction processes of dietary fiber, Food Eng Rev 8 (2016) 251–271, https://doi.org/10.1007/s12393-015-9134-y.
[83] A. Karim, Z. Raji, Y. Habibi, S. Khalloufi, A review on the hydration properties of dietary fibers derived from food waste and their interactions with other ingredients: opportunities and challenges for their application in the food industry, Crit Rev Food Sci Nutr (2023) 1–35, https://doi.org/10.1080/10408398.2023.2243510.
[84] K. Slater, Comfort properties of textiles, Text, Program 9 (1977) 1–70, https://doi.org/10.1080/00405167.1977.10750095.
[85] E. Pakdel, M. Naebe, L. Sun, X. Wang, Advanced functional fibrous materials for enhanced thermoregulating performance, ACS Appl Mater Interfaces 11 (2019) 13039–13057, https://doi.org/10.1021/acsami.8b19067.
[86] K.M. Salleh, N.A.Z. Armir, N.S.N. Mazlan, C. Wang, S. Zakaria, Cellulose and its derivatives in textiles: primitive application to current trend, in: Fundam. Nat. Fibres Text, Elsevier. 2021, pp. 33–63, https://doi.org/10.1016/B978-0-12-821483-1.00014-0.
[87] J. Shokri, K. Adibkia, Application of cellulose and cellulose derivatives in pharmaceutical industries, in: Cellul. Pharm. Electron. Appl., IntechOpen, 2013, https://doi.org/10.5772/55178.316.
[88] R.I. Mahato, A.S. Narang, Pharmaceutical Dosage Forms and Drug Delivery: Revised and Expanded, CRC Press. 2017, https://doi.org/10.1201/9781315156941.728.
[89] B. Sun, M. Zhang, J. Shen, Z. He, P. Fatehi, Y. Ni, Applications of cellulose-based materials in sustained drug delivery systems, Curr Med Chem. 26 (2019) 2485–2501, https://doi.org/10.2174/0929867324666170705143308.
[90] W.Y. Hamad, T.Q. Hu, Structure–process–yield interrelations in nanocrystalline cellulose extraction, Can J Chem Eng 88 (2010) 392–402, https://doi.org/10.1002/cjce.20298.
[91] A. Devarajan, S. Markutsya, M.H. Lamm, X. Cheng, J.C. Smith, J.Y. Baluyut, Y. Kholod, M.S. Gordon, T.L. Windus, Ab initio study of molecular interactions in cellulose Iα, J Phys Chem B 117 (2013) 10430–10443, https://doi.org/10.1021/jp406266u.
[92] R. Mao, N. Meng, W. Tu, T. Peijs, Toughening mechanisms in cellulose nanopaper: the contribution of amorphous regions, Cellulose 24 (2017) 4627–4639, https://doi.org/10.1007/s10570-017-1453-0.
[93] G. Gayathri, G. Srinikethan, Bacterial cellulose production by *K. saccharivorans* BC1 strain using crude distillery effluent as cheap and cost effective nutrient medium, Int J Biol Macromol 138 (2019) 950–957, https://doi.org/10.1016/j.ijbiomac.2019.07.159.
[94] Y. Cao, S. Lu, Y. Yang, Production of bacterial cellulose from byproduct of citrus juice processing (citrus pulp) by *Gluconacetobacter hansenii*, Cellulose 25 (2018) 6977–6988, https://doi.org/10.1007/s10570-018-2056-0.
[95] S.S.Z. Hindi, Some crystallographic properties of cellulose I as affected by cellulosic resource, smoothing, and computation methods, Cellulose 6 (2017) 732–752.